

Article

Theoretical Study on Specific Loss Power and Heating Temperature in CoFe_2O_4 Nanoparticles as Possible Candidate for Alternative Cancer Therapy by Superparamagnetic Hyperthermia

Costica Caizer

Department of Physics, Physics Faculty, West University of Timisoara, Bv. V. Pärvan No. 4, 300223 Timisoara, Romania; costica.caizer@e-uvt.ro

Abstract: In this paper, we present a theoretical study on the maximum specific loss power in the admissible biological limit $(P_{SM})_1$ for CoFe_2O_4 ferrimagnetic nanoparticles, as a possible candidate in alternative and non-invasive cancer therapy by superparamagnetic hyperthermia. The heating time of the nanoparticles (Δt_0) at the optimum temperature of approx. 43°C for the efficient destruction of tumor cells in a short period of time, was also studied. We found the maximum specific loss power P_{SM} (as a result of superparamagnetic relaxation in CoFe_2O_4 nanoparticles) for very small diameters of the nanoparticles (D_0), situated in the range of 5.88–6.67 nm, and with the limit frequencies (f_1) in the very wide range of values of 83–1000 kHz, respectively. Additionally, the optimal heating temperature (T_0) of 43°C was obtained for a very wide range of values of the magnetic field H , of 5–60 kA/m, and the corresponding optimal heating times (Δt_0) were found in very short time intervals in the range of ~ 0.3 –44 s, depending on the volume packing fraction (ϵ) of the nanoparticles. The obtained results, as well as the very wide range of values for the amplitude H and the frequency f of the external alternating magnetic field for which superparamagnetic hyperthermia can be obtained, which are great practical benefits in the case of hyperthermia, demonstrate that CoFe_2O_4 nanoparticles can be successfully used in the therapy of cancer by superparamagnetic hyperthermia. In addition, the very small size of magnetic nanoparticles (only a few nm) will lead to two major benefits in cancer therapy via superparamagnetic hyperthermia, namely: (i) the possibility of intracellular therapy which is much more effective due to the ability to destroy tumor cells from within and (ii) the reduced cell toxicity.



Citation: Caizer, C. Theoretical Study on Specific Loss Power and Heating Temperature in CoFe_2O_4 Nanoparticles as Possible Candidate for Alternative Cancer Therapy by Superparamagnetic Hyperthermia. *Appl. Sci.* **2021**, *11*, 5505. <https://doi.org/10.3390/app11125505>

Academic Editor: Yurii K. Gun'ko

Received: 16 May 2021

Accepted: 10 June 2021

Published: 14 June 2021

Publisher's Note: MDPI stays neutral with regard to jurisdictional claims in published maps and institutional affiliations.



Copyright: © 2021 by the author. Licensee MDPI, Basel, Switzerland. This article is an open access article distributed under the terms and conditions of the Creative Commons Attribution (CC BY) license (<https://creativecommons.org/licenses/by/4.0/>).

Keywords: cobalt ferrite nanoparticles; specific loss power; superparamagnetic hyperthermia; alternative cancer therapy

1. Introduction

Superparamagnetic hyperthermia (SPMHT) for alternative and noninvasive cancer therapy uses magnetic nanoparticles that have a superparamagnetic behavior in an external magnetic field [1–7]. By the effect of magnetic relaxation [2,8,9] in an alternating magnetic field with amplitude H and frequency f of hundreds of kHz, the magnetic nanoparticles are heated [1]. Thus, by introducing magnetic nanoparticles into the tumor by various techniques using modern nanobiotechnology [10], and then heating them by magnetic relaxation following the application of the magnetic field from the outside, the temperature of approx. 43°C required for the destruction of tumor cells can be obtained. So, superparamagnetic hyperthermia uses the natural thermal effect to destroy tumor cells, being a new technique, alternative to classical techniques (chemo- and radiotherapy), and also non-invasive, having low or even no toxicity [7,10–12] compared with classical techniques that have a high degree of toxicity on the body.

Today, superparamagnetic hyperthermia is considered as the method of the future in cancer therapy due to the very promising results obtained so far both in vitro, in vivo

and in clinical trials [7,10,11,13–28]. However, the effectiveness and efficiency of superparamagnetic hyperthermia in destroying tumor cells depends very much on the magnetic nanoparticles used for it. Most viable results have been obtained so far by using Fe_3O_4 nanoparticles (magnetite) [13–19,29–39], but also other magnetically soft ferromagnetic nanoparticles (which have low magnetic anisotropy) [40–51].

However, magnetite nanoparticles, although they seem to be the most suitable in terms of magnetic characteristics and efficiency in obtaining a high specific dissipated power, they have a major disadvantage, namely: the size of the nanoparticles which is too large, in the range of 14–17 nm, for obtaining superparamagnetic hyperthermia in optimal conditions [1,28,52,53]. This can cause problems of cellular toxicity, and to reduce it requires the use of low concentrations of nanoparticles in therapy, which will decrease the effectiveness of superparamagnetic hyperthermia. Elimination of this major drawback could be done using CoFe_2O_4 ferrite nanoparticles, by replacing Fe^{2+} ions in the lattice of magnetite ($\text{Fe}^{3+}[\text{Fe}^{2+}, \text{Fe}^{3+}]\text{O}_4^{2-}$ [54] with Co^{2+} ions in the ratio of 1:1 ($\text{Fe}^{3+}[\text{Co}^{2+}, \text{Fe}^{3+}]\text{O}_4^{2-}$). Thus, an inverse spinel will be obtained as in the case of magnetite having the saturation magnetization (425 kA/m) close to that of the magnetite (480 kA/m), but a considerably higher magnetic anisotropy: 200 kJ/m³ [55] compared to only 11 kJ/m³ [54] in the case of magnetite. The slight decrease in magnetization in the case of cobalt ferrite will not significantly influence in terms of superparamagnetic hyperthermia, but the large increase in magnetic anisotropy (of ~18 times) will radically change the hyperthermic behavior, both in terms of the specific loss power as well as of the heating temperature of the nanoparticles. Thus, the high magnetic anisotropy in the case of cobalt ferrite nanoparticles leads to obtaining a maximum heating rate for very small nanoparticles, of the order of a few nm [1]. The reduced size of CoFe_2O_4 nanoparticles will have at least two major beneficial effects in the superparamagnetic hyperthermia of tumors: (i) the reduction of cellular toxicity [12] due to reduced nanoparticle size, and (ii) the possibility of intracellular therapy by superparamagnetic hyperthermia [56]. These are two very important issues to consider in magnetic hyperthermia in addition to increasing the specific loss power, on which the effectiveness of tumor therapy greatly depends. Therefore, cobalt ferrite nanoparticles are currently of particular scientific interest to be applied in magnetic hyperthermia for cancer therapy [5,57–66].

As a result, a systematic and in-depth study of the superparamagnetic hyperthermia with CoFe_2O_4 nanoparticles is required in order to understand its use for the therapy of tumors with increased efficiency and low or lack of toxicity. Only a few studies were done so far on the use of cobalt ferrite nanoparticles in magnetic hyperthermia compared to those related to magnetite, for example. Thus, the optimal conditions in which superparamagnetic hyperthermia can be obtained with CoFe_2O_4 nanoparticles were not yet determined in order to obtain the maximum specific loss power that leads to an increase in the efficacy of cobalt ferrite nanoparticles in tumor therapy and, at the same time, to a reduction in the heating time of the nanoparticles at an optimal temperature of 43 °C in order not to affect healthy tissues.

Therefore, in this paper, we present a systematic and complete study on the maximum specific loss power $(P_{\text{SM}})_l$ within the allowable biological limit that can be obtained in superparamagnetic hyperthermia using CoFe_2O_4 ferrite nanoparticles a promising candidate in cancer therapy with increased efficacy on tumors. We also determined the optimal heating time (Δt_0) of the nanoparticles for the temperature of 43 °C in superparamagnetic hyperthermia with CoFe_2O_4 nanoparticles in order to obtain the maximum efficiency in destroying the tumor cells within the admissible biological limit so as not to damage healthy tissues. At the same time, we established the maximum value of the magnetic field up to which the linear approximation can be applied in superparamagnetic hyperthermia in the case of CoFe_2O_4 nanoparticles.

2. Basic Theoretical Aspects

The standard physical observables that indicate if different magnetic nanoparticles can be used in superparamagnetic hyperthermia to destroy tumor cells are: specific loss power P_s (or denoted symbolic SLP) and heating rate of nanoparticles $\Delta T_i / \Delta t$, where T_i is the temperature and t is the time, having in view that the specific absorption rate (SAR) [67] for an adiabatic system is

$$SAR = c\Delta T_i / \Delta t \quad (1)$$

where c is the specific heat capacity of the nanoparticles.

The specific loss power can be expressed by the formula [1,53]

$$P_s = \frac{3\pi\mu_0\chi_i}{\rho\zeta} \left(\coth\zeta - \frac{1}{\zeta} \right) \frac{2\pi f\tau}{1 + (2\pi f\tau)^2} fH^2 \quad (2)$$

where μ_0 is the magnetic permeability of vacuum ($4\pi \times 10^{-7}$ H/m), f and H are the frequency and the amplitude of magnetic field, ρ is the density of nanoparticle material. The observable ζ in the above formula is the parameter of the Langevin function [68], expressed as a function of the diameter of the nanoparticles (D) considered spherical.

$$\zeta = \frac{\pi\mu_0 M_s D^3}{6k_B T} H \quad (3)$$

that describing the magnetization of magnetic nanoparticles (M) in the external magnetic field H [69],

$$M = M_{sat} \left(\coth\zeta - \frac{1}{\zeta} \right) \quad (4)$$

where M_{sat} is the saturation magnetization of the nanoparticle system. The observable ζ is the initial magnetic susceptibility of magnetic nanoparticles [4,53], which is given by the formula:

$$\chi_i = \frac{\varepsilon\pi\mu_0 M_s^2 D^3}{18k_B T} \quad (5)$$

and strongly depends on the diameter of the magnetic nanoparticles (the diameter at the third power). The observable τ in Equation (2) is the Néel magnetic relaxation time [2]

$$\tau = \tau_0 \exp\left(\frac{\pi K D^3}{6k_B T}\right) \quad (6)$$

where τ_0 is a time constant with a value of 10^{-9} [70].

Formula given by Equation (2) was determined by taking into account the dependence of static magnetic susceptibility on the external magnetic field applied when reaching high values and the magnetic susceptibility can no longer be considered constant and equal to the initial magnetic susceptibility (χ_i) [53].

In small amplitude fields the formula is simplified, being reduced to [53]

$$P_s = \frac{\pi\mu_0\chi_i}{\rho} \frac{2\pi f\tau}{1 + (2\pi f\tau)^2} fH^2 \quad (7)$$

Taking into account the specific absorption rate given by Equation (1) and the specific loss power in an adiabatic system ($SAR = P_s$) given by Equation (2) (or Equation (7)) it is possible to obtain the heating temperature ΔT_h of the nanoparticles in a finite time interval Δt .

$$\Delta T_h = \frac{1}{c} P_s \Delta t \quad (8)$$

In magnetic hyperthermia of tumors, the heating temperature must reach approx. 43 °C in a short period of time in order to be effective on tumor cells, leading to their destruction at least by cellular apoptosis [7,10], and not to affect healthy cells. However,

heating temperatures during magnetic hyperthermia can increase to values higher than 43 °C. In such cases, automatic control systems with an electronic reaction of the magnetic field generator (reverse reaction) can be used which allows limiting and maintaining the heating temperature constant at the required value of 43 °C.

In conclusion, if during the process of heating the magnetic nanoparticles in superparamagnetic hyperthermia a temperature of least 42.5–43 °C is obtained in a short period of time so that the healthy cells are not affected, then those nanoparticles could be successfully used in cancer therapy via superparamagnetic hyperthermia.

3. Results and Discussion

3.1. Characteristic Observables of CoFe₂O₄ Nanoparticles and Study Method

The specific parameters of interest of the magnetic material of the CoFe₂O₄ ferrimagnetic nanoparticles are shown in Table 1. These are: spontaneous magnetization of the material M_s , magnetocrystalline anisotropy constant K , material density ρ and specific heat c [1,54,55].

Table 1. Characteristic observables of the CoFe₂O₄ ferrite nanoparticles and parameters of magnetic field.

M_s ($\times 10^3$ A m ⁻¹)	K ($\times 10^3$ J m ⁻³)	ρ ($\times 10^3$ kg·m ⁻³)	c (Jkg ⁻¹ K ⁻¹)	ϵ	H ($\times 10^3$ A m ⁻¹)	f ($\times 10^3$ Hz)	D ($\times 10^{-9}$ m)
425	200	5.29	700	0.01–0.15	5–180	50–1000	1–20

For the study of the specific loss power and heating temperature of CoFe₂O₄ nanoparticles, we used a professional 3D powerful software tool for calculation. We used the formulas in Section 1, and a spatial graphical representation in order to capture all the details through a simultaneous representation of the observables of interest as a function of two variables: the parameters of the harmonic alternating magnetic field (amplitude H and frequency f) and the basic characteristics of the magnetic nanoparticles (diameter D and volume packing fraction ϵ) given in Table 1. Given that, in practice, magnetic hyperthermia is most often in the range of 100–500 kHz and for magnetic fields in the range of 10–40 kA/m, we have extended these ranges to study possible valid results that could be obtained outside the ranges used up to now. Additionally, for the diameter of nanoparticles D , for the same reason, the range of 1–20 nm was chosen, considering the known values for magnetite and γ -Fe₂O₃ nanoparticle diameters (~15–20 nm). For the spontaneous magnetization and magnetic anisotropy constant in Table 1 we considered the standard values for CoFe₂O₄ ferrite [54,55], having in view the following reasons. In the case of magnetic nanoparticles, and even more for ferromagnetic and ferrimagnetic ones in which the exchange and superexchange interactions are strong, for small sizes of nanoparticles an important contribution of surface effects (spin canting, broken exchange bonds, etc.) can occur to magnetic saturation [71–73] and magnetic anisotropy [74–76], depending on the type and size of nanoparticles. This contribution can be manifested by a surface magnetic anisotropy [77–80] and decreased magnetic saturation [71–73,81]. Additionally, if the magnetic nanoparticles are not spherical there may be an important contribution of the shape of the nanoparticles to magnetic anisotropy if the nanoparticles deviate much from the spherical shape (e.g., magnetic nanoparticles are elongated) [82]. Thus, for magnetic anisotropy an effective magnetic anisotropy constant (K_{eff}) should be considered as a contribution of the magnetocrystalline anisotropy constant (K), the surface anisotropy constant (K_s) and the shape anisotropy constant (K_{sh}) ($K_{\text{eff}} = K + K_s + K_{\text{sh}}$) [78,80]. However, in the case of our study we considered spherical nanoparticles ($K_{\text{sh}} = 0$), a condition fulfilled in most practical cases. Additionally, in the case of cobalt ferrite nanoparticles, the magnetocrystalline anisotropy constant ($K = 2 \times 10^5$ J/m³ [54]) is much larger than the surface anisotropy constant (K_s), which in general can be found in the range $1\text{--}5 \times 10^4$ J/m³ [78–80], depending on the size and type of nanoparticles. Therefore, in the case of CoFe₂O₄ ferrite nanoparticles the most important contribution to magnetic

anisotropy is given by the magnetocrystalline component ($K_{\text{eff}} \sim K$) [83], as we will consider in this paper (Table 1) [55]. Additionally, the surface effects and spins disorder in surface layer of nanoparticles can significantly reduce the spontaneous/saturation magnetization at room temperature. However, the concrete value of the decrease of spontaneous/saturation magnetization depends on many other factors, besides the size of the nanoparticles, such as the type of magnetic material, the preparation conditions of the sample, the surfactant or not of the nanoparticles, different heat treatments, previous history of sample, etc. Therefore, it is difficult to predict an exact value of the spontaneous magnetization of nanoparticles. Thus, in order not to introduce ambiguities in this theoretical study, we consider in the calculations the standard value of the spontaneous magnetization (M_s) at room temperature (20 °C) of the CoFe_2O_4 ferrite (Table 1) [54]. Of course, in the case of concrete applications, it is beneficial to determine experimentally a priori the values of spontaneous/saturation magnetization and effective magnetic anisotropy of nanoparticles for better accuracy.

In our study, we considered two fundamental observables used in superparamagnetic hyperthermia: (i) the specific loss power (P_s) (Equation (2) with Equations (3), (5)–(7)) and (ii) the heating temperature (T_h) (Equation (8)) for CoFe_2O_4 nanoparticles, which are key parameters in the analysis of the efficacy and effectiveness of superparamagnetic hyperthermia for cancer therapy.

3.2. The Maximum Specific Loss Power in the Case of Superparamagnetic Hyperthermia with CoFe_2O_4 Nanoparticles

The most important observable that allows the anticipation of the characteristics that CoFe_2O_4 ferrimagnetic nanoparticles must have in order to be successfully used in superparamagnetic hyperthermia for the destruction of tumor cells is the specific loss power P_s (or SLP). Using Equation (2) and Equations (3), (5) and (6), with the values of the characteristic parameters in Table 1, the specific loss power P_s was calculated as a function of the diameter of nanoparticles (D) and the characteristic observables of magnetic field: frequency (f) and amplitude (H). For this it was taken into account that the size of magnetic nanoparticles is a key parameter in magnetic hyperthermia, therefore it was considered primarily the dependence of the specific loss power P_s on the diameter D of nanoparticles.

Thus, the 3D dependence of the specific loss power (P_s) in the CoFe_2O_4 ferrimagnetic nanoparticles as a function of the nanoparticle diameter (D) and the frequency of the magnetic field (f) for the values included in the domains $D = 1\text{--}20$ nm and $f = 100\text{--}1000$ kHz (Table 1), and for volume packing fraction $\epsilon = 0.15$, having as parameter the amplitude of magnetic field H (in the range specified in Table 1), is shown in Figure 1. Here two values for H were considered: 15 kA/m (Figure 1a) and 30 kA/m (Figure 1b).

The obtained results show four very important aspects for the subsequent and efficient application of superparamagnetic hyperthermia:

- (i) The specific loss power P_s has a narrow maximum (P_{sM}) for a very small value of the diameter (D) of the CoFe_2O_4 nanoparticle of approx. 6–6.5 nm. This result is in good agreement with the one obtained in [1,67].

However, the result is very different from that obtained for the magnetite nanoparticles (Fe_3O_4), where the maximum specific loss power was obtained at a nanoparticle diameter of ~16–17 nm [28,53]. This high difference in the diameters of magnetic nanoparticles is due to the very high magnetic anisotropy of cobalt ferrite, which has a much higher magnetocrystalline anisotropy constant (200 kJ/m³) [55] than that of magnetite (11 kJ/m³) [54], which makes the maximum loss power to be obtained at significantly lower values of the CoFe_2O_4 nanoparticles diameter.

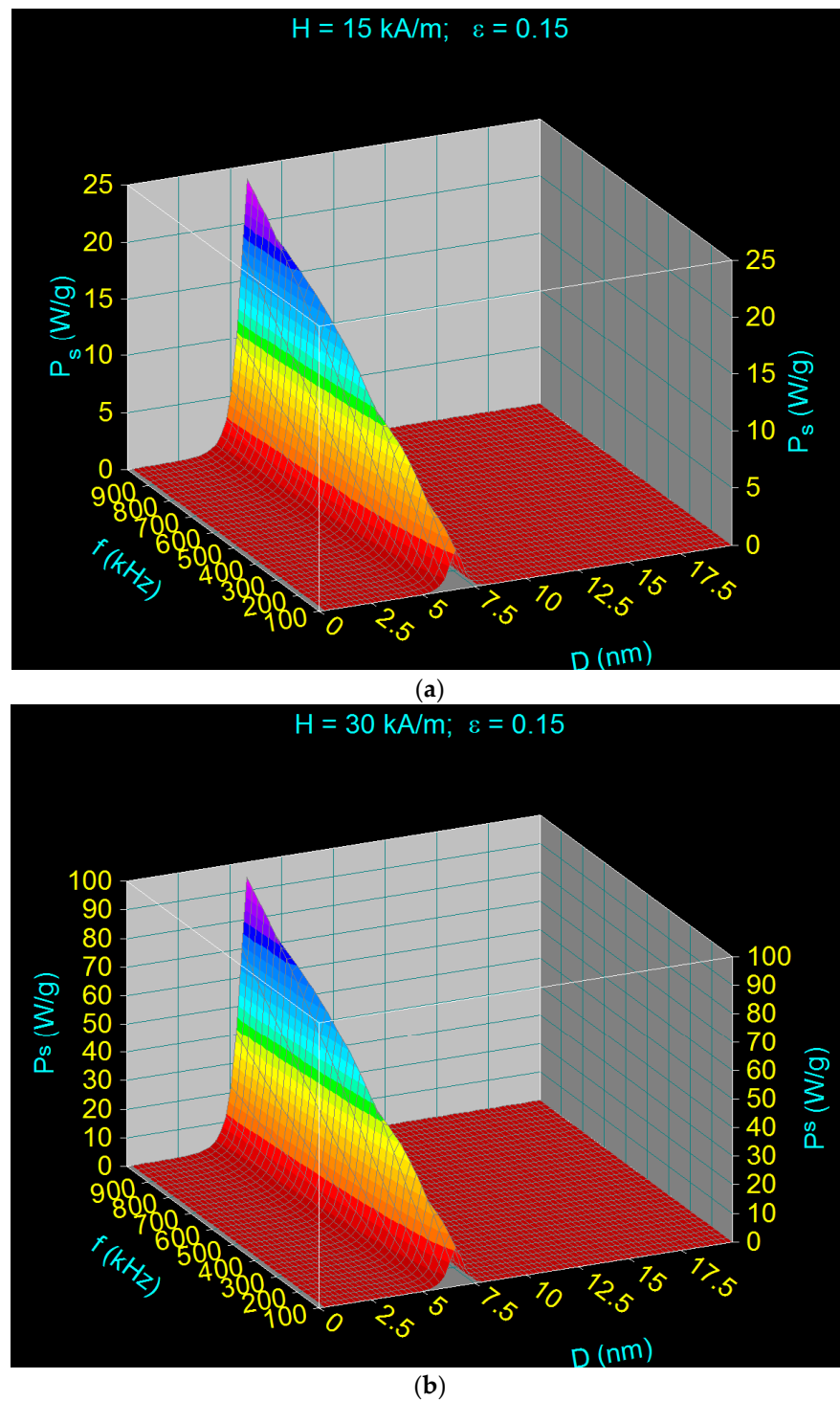


Figure 1. The specific loss power (P_s) as a function of CoFe_2O_4 nanoparticles diameter (D) and magnetic field frequency (f) for amplitude of the magnetic field of (a) 15 kA/m and (b) 30 kA/m.

The fact that CoFe_2O_4 nanoparticles are very small is a major advantage in terms of magnetic hyperthermia, which can be achieved intracellularly, leading to a more efficient destruction of tumor cells from within. The nanoparticles being so small can easily penetrate through the phospholipids membrane inside the cells (cytoplasm or even the nucleus), thus destroying them more efficiently from inside.

- (ii) There is a dependence of the maximum specific loss power P_{sM} on the diameter of the magnetic nanoparticles D as a function of the frequency of the magnetic field f

(Figure 2), namely: the maximum power shifts from higher values to lower values of the nanoparticle diameter when the magnetic field frequency increases from 100 kHz to 1000 kHz. Table 2 shows some values for the diameters of CoFe_2O_4 nanoparticles for which the maximum loss power is obtained for the frequency range limits (100 kHz and 1000 kHz) as well as at the mid-value of those limits (500 kHz).

Table 2. The values of maximum specific loss power (P_{sM}) and the corresponding diameter of CoFe_2O_4 nanoparticles (D_M) for three frequencies in the range of 100–1000 kHz, and $H = 15 \text{ kA/m}$ and $\varepsilon = 0.15$.

P_{sM} (W/g)	f (kHz)	D_M (nm)
3.46	100	6.62
13.64	500	6.12
24.13	1000	5.88

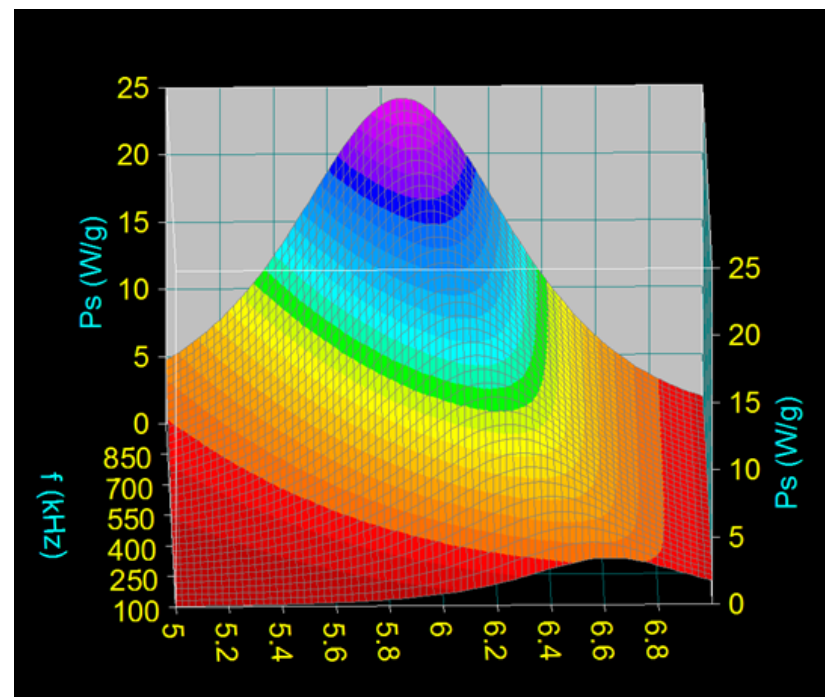


Figure 2. The variation of the position of maximum specific loss power (P_{sM}) with the frequency of magnetic field (f) and diameter of CoFe_2O_4 nanoparticles (D) in nanometers range.

Therefore, given the size dependencies of the 3rd power of the nanoparticle diameter in the initial magnetic susceptibility (Equation (5)), the Langevin parameter (Equation (3)) and the magnetic relaxation time (Equation (6)), for a precise calculation we must take into account the diameter values corresponding to the frequencies identified (as in Table 2) when calculating the maximum loss power P_{sM} (Equation (2)), and then when calculating the heating temperature of the nanoparticles ΔT_h (Equation (8)). A small deviation of the nanoparticle diameter from those values identified to be corresponding to the maximum will lead to lower values of the specific loss power, and implicitly of the heating temperature.

(iii) The maximum loss power increases both with the amplitude and the frequency of magnetic field as shown in Figure 3. However, the increase is more accentuated with the increase of the magnetic field amplitude (see Figure 1a,b). However, for the magnetic fields higher than 60–70 kA/m there is a limiting effect (saturation) of increasing the specific loss power at frequencies above 600–700 kHz.

- (iv) The specific loss power for CoFe_2O_4 nanoparticles is significantly lower than in the case of magnetite nanoparticles. However, if the power obtained under these conditions were sufficient to heat the nanoparticles to an optimum temperature of $\sim 43^\circ\text{C}$, and in a relatively short period of time (see Section 3.5), then the reduced power would not come as a disadvantage in the use of CoFe_2O_4 nanoparticles in superparamagnetic hyperthermia for tumor therapy. In addition, we've shown a major advantage in point (ii), regarding intracellular therapy, which will increase the effectiveness of CoFe_2O_4 nanoparticles in the hyperthermic destruction of tumor cells, much more efficiently from within.

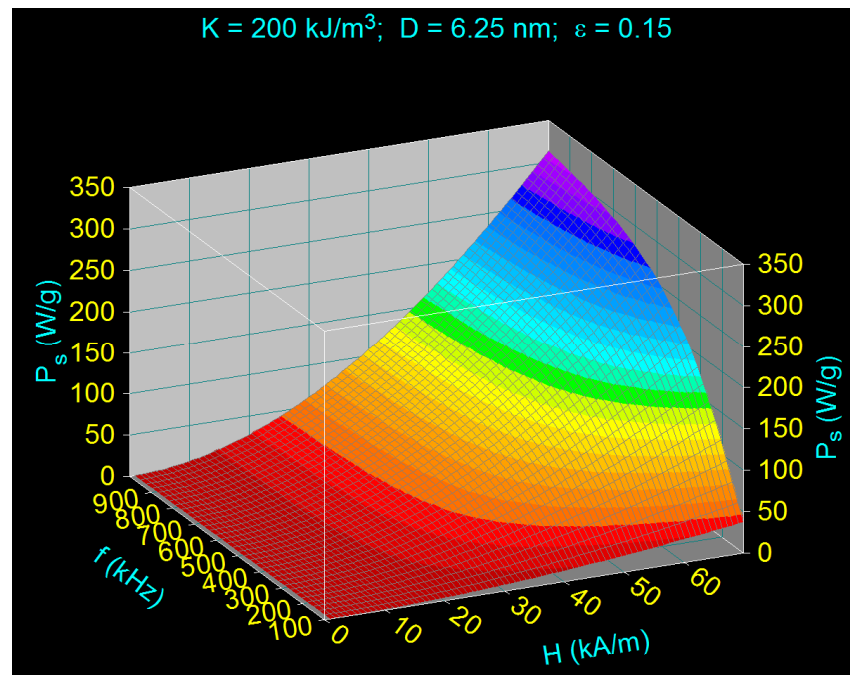


Figure 3. The variation of specific loss power (P_s) as a function of the amplitude (H) and frequency (f) of magnetic field for the diameter (D) of the CoFe_2O_4 nanoparticles of 6.25 nm.

However, there is another important question that arises in these conditions, as follows: what is the appropriate magnetic field in which the formula of specific loss power in the linear approximation can be used? A detailed answer will be given in the next paragraph.

3.3. The Specific Loss Power in the Linear Approximation

3.3.1. Maximum Specific Loss Power

Using the formulas for the calculation of the specific loss power P_s given by Equation (2) and Equation (7), the calculations made for the maximum specific loss power (P_{sM}) at the frequency of 500 kHz for two relatively distant magnetic field values, one usual of (a) 15 kA/m and the other relatively high (b) 60 kA/m, lead to the results shown in Figure 4. Using Equation (7) we obtained the diagrams (a1) for the magnetic field of 15 kA/m and the diagram (b1) for the magnetic field of 60 kA/m. Using Equation (2) we obtained the diagrams (a2) for 15 kA/m and (b2) for 60 kA/m. The results show that there are no noticeable differences between the maximums of the specific loss powers P_{sM} obtained in the case of Equation (2) and for the higher magnetic field of 60 kA/m (Figure 4b2).

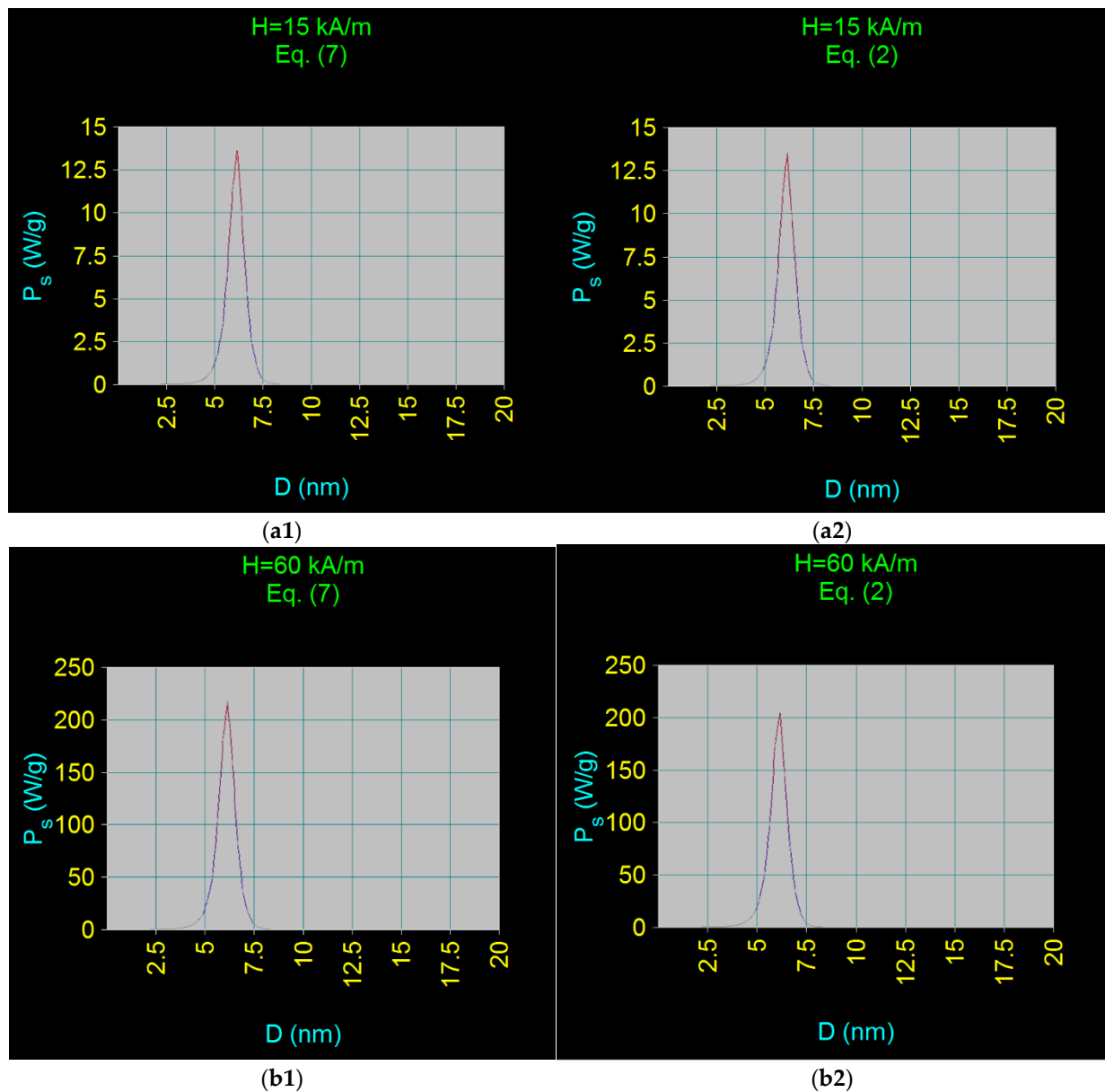


Figure 4. The specific loss power (P_s) as a function of CoFe_2O_4 nanoparticles diameter (D) calculated at the magnetic field frequency (f) of 500 kHz, using: (a1) Equation (7) and the magnetic field amplitude $H = 15$ kA/m, (b1) Equation (7) and $H = 60$ kA/m, (a2) Equation (2) and $H = 15$ kA/m, and (b2) Equation (2) and $H = 60$ kA/m.

The explanation for this behavior which is very different from the case of magnetite is the following: Co ferrite nanoparticles have high magnetic anisotropy [55,83] which leads to a very small size of the nanoparticle diameter D which determines the maximum specific loss power, as previously shown (Figure 1). The small size of the nanoparticles also causes a low magnetic susceptibility (χ_0), which also varies very little with the increase of the magnetic field even when using very large magnetic fields of approx. 100 kA/m, as seen in Figure 5.

Calculating the maximum loss powers (P_{sM}) for those two cases (as in Figure 4), using Equations (2) and (7), we find that the differences between them appear only at large values of the magnetic field, over ~ 70 kA/m as shown in Figure 6. The yellow curve represents the variation of the maximum specific loss power with the increase of the magnetic field up to the value of 100 kA/m in the linear approximation given by Equation (7), considering the magnetic susceptibility constant and equal to the initial one (χ_i). The green curve represents the maximum specific loss power calculated using the formula given by Equation (2), when

the susceptibility depends on the magnetic field. The maximum specific loss powers were calculated at a frequency of 500 kHz and for the corresponding nanoparticle diameter of 6.12 nm.

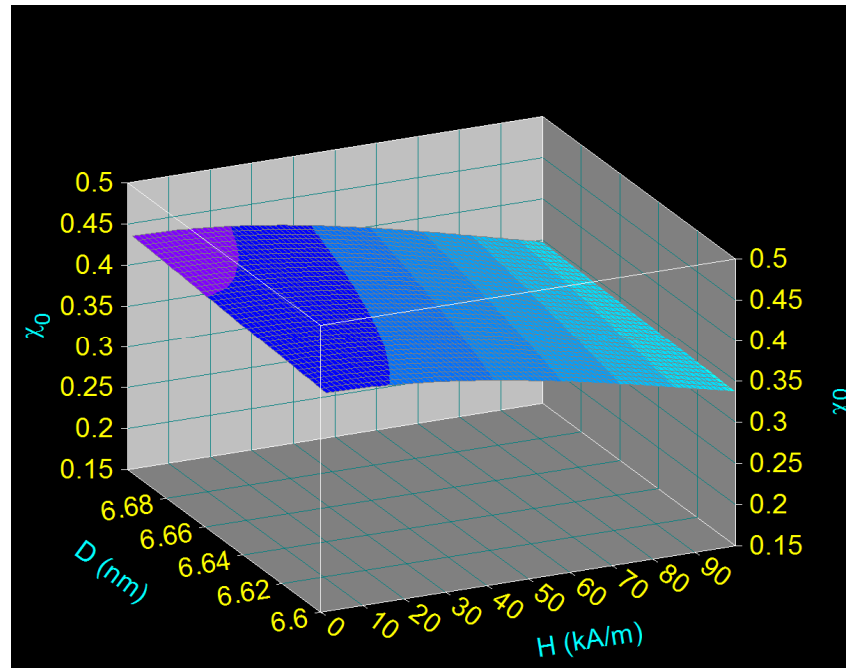


Figure 5. The variation of magnetic susceptibility of CoFe_2O_4 nanoparticles as a function of the amplitude of magnetic field H up to 100 kA/m, for the diameters of nanoparticles of 6.6–6.7 nm.

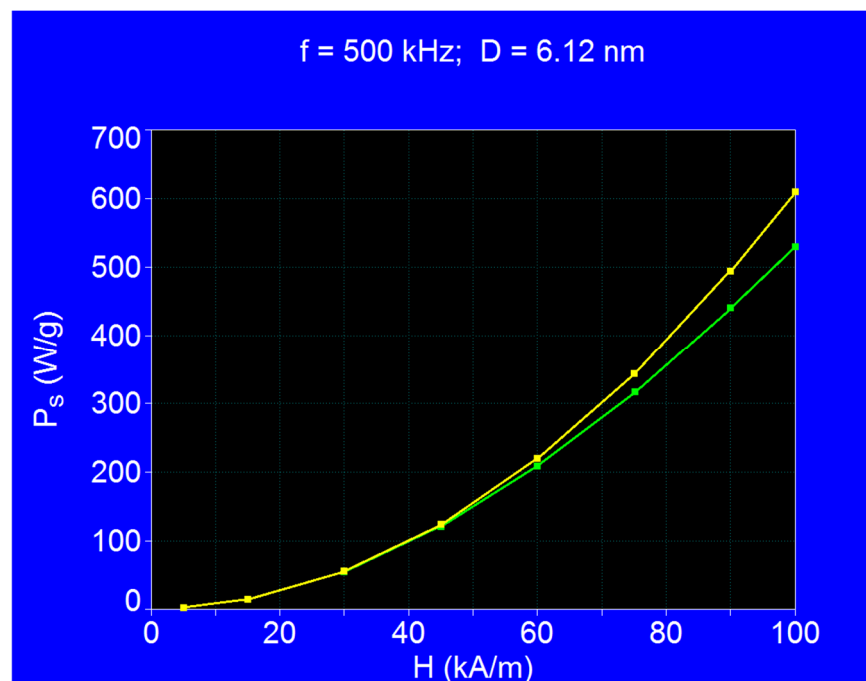


Figure 6. The dependence of the maximum specific loss power (P_{sM}) on the magnetic field (H) for CoFe_2O_4 nanoparticles, calculated at the frequency (f) of 500 kHz using Equation (7) (yellow curve) and Equation (2) (green curve).

The explanation for this behavior in the case of CoFe_2O_4 nanoparticles which is very different from that of magnetite is given in the next section.

3.3.2. Magnetic Behavior of Small CoFe_2O_4 Nanoparticles and Linearity of Magnetization

When calculating the magnetization (M) in the case of CoFe_2O_4 nanoparticles using Equation (4), where the parameter of the Langevin function is given by Equation (3), for an average nanoparticle diameter of ~ 6 nm we obtained the curve $M = f(H)$ shown in Figure 7a. In our calculus, we took into account the saturation magnetization of the nanoparticles expressed by

$$M_{sat} = \varepsilon M_s \quad (9)$$

where ε is the magnetic packing fraction (considered 0.15 as in all calculations made until now) and M_s is spontaneous magnetization [54] (Table 1). The magnetization was calculated up to a magnetic field close to saturation (500 kA/m) in order to register the Langevin type variation of the magnetization.

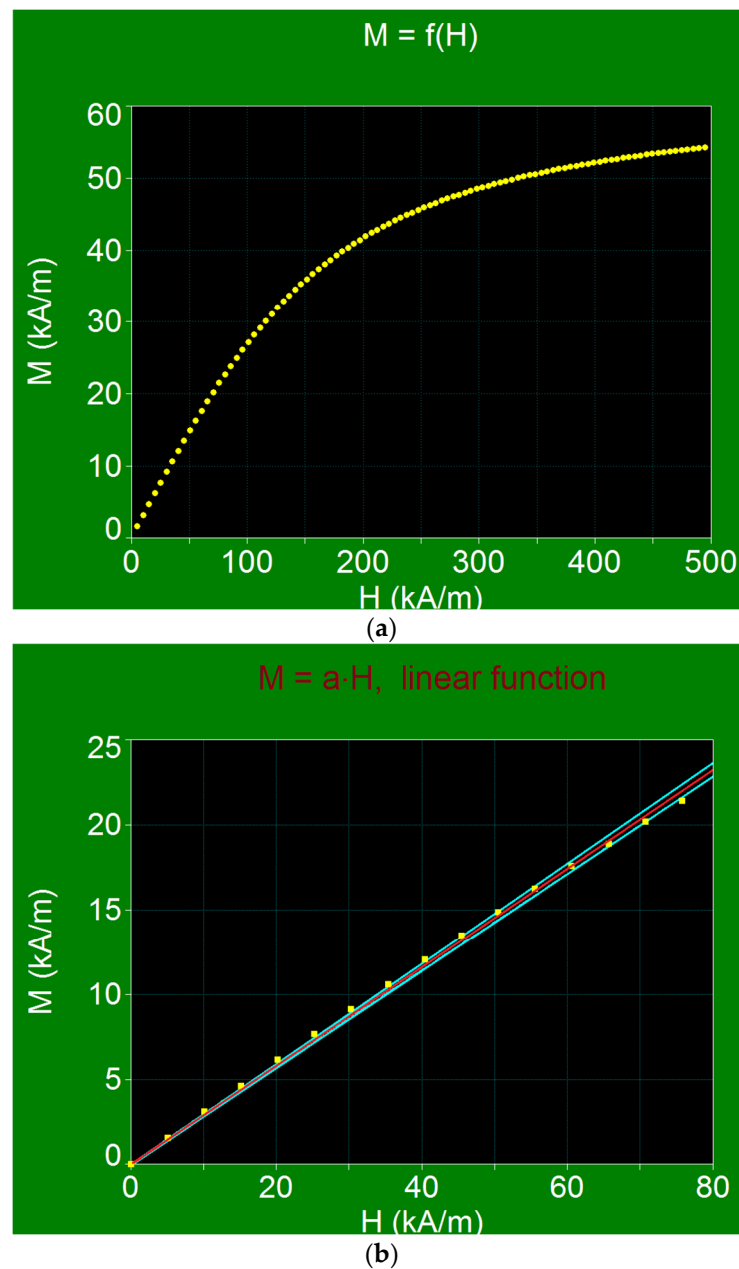


Figure 7. The magnetization M as a function of magnetic field H for CoFe_2O_4 nanoparticles in (a) high and (b) low magnetic field.

Using the data fit technique obtained with professional software and using a linear function in the range of low fields, we find a very good linear dependence (red line) of magnetization with the field (Figure 7b): $M = \alpha H$, where α is the slope of the line. Moreover, this linear dependence is well fulfilled up to large magnetic fields of ~ 60 kA/m. In Figure 7b the confidence interval is marked with the light blue color.

Thus, the results obtained above show that the linear approximation in the case of CoFe_2O_4 nanoparticles can be used up to large magnetic fields (up to 60 kA/m), compared to magnetite, for example, where the field did not exceed 5 kA/m [53]. The obtained result is also in agreement with the one shown in Figure 6, where it is clearly observed that up to the magnetic field of ~ 60 kA/m the maximum specific loss power P_{sM} can be calculated in the linear approximation, and the Equation (7) can be used in this case instead of the Equation (2).

All these results shows that the calculations for determining the specific loss power in the case of CoFe_2O_4 nanoparticles are greatly simplified. Additionally, this is a great advantage in the case of the practical implementation of superparamagnetic hyperthermia because it is no longer necessary to know the magnetic susceptibility (χ_0) as the nonlinear field function $\chi_0 = f(H)$,

$$\chi_0 = \chi_i \frac{3}{\zeta} \left(\coth \zeta - \frac{1}{\zeta} \right) \quad (10)$$

where ζ and χ_i are given by the Equations (3) and (5).

This very different magnetic behavior in the case of CoFe_2O_4 nanoparticles is also due to the small size (diameter) of the nanoparticles that are used in superparamagnetic hyperthermia to obtain the maximum specific loss power (Figure 1). The small size of CoFe_2O_4 nanoparticles is due to their very large magnetic anisotropy.

Under these conditions, the parentheses in Equation (4) can be approximated by

$$\coth \zeta - \frac{1}{\zeta} \cong \frac{1}{3} \zeta \quad (11)$$

and, therefore, the magnetic susceptibility used can be approximated with the initial one χ_i ,

$$\chi_0 \cong \chi_i = \text{const.} \quad (12)$$

which is constant (for a given diameter of the nanoparticle (Equation (3))).

3.4. Maximum Specific Loss Power in Superparamagnetic Hyperthermia under Optimal Conditions and within Biologically Permissible Limits

The efficiency of the method of superparamagnetic hyperthermia with CoFe_2O_4 ferrimagnetic nanoparticles must be analyzed within the biologically permissible limits of a magnetic field that does not affect healthy tissues. Thus, taking into account the values for the amplitude and frequency of the magnetic field corresponding to the admissible biological limit [84],

$$H \cdot f_l \leq 5 \times 10^9 \text{ (Am}^{-1}\text{Hz)} \quad (13)$$

where f_l is the limit frequency, and using the 3D representations for the specific loss powers as in Figure 1, the maximum values of P_s and the corresponding optimal diameters (D_{op}) of the CoFe_2O_4 nanoparticles were determined that lead to a maximum power $(P_{sM})_l$. The values of $(P_{sM})_l$ have been determined for a very wide range of values of the amplitude of the magnetic field (5–180 kA/m). The identified values are shown in Table 3.

Table 3. The values of maximum specific loss power ($(P_{sM})_l$) for the optimal diameter (D_o) of CoFe_2O_4 nanoparticles at the admissible biological limit for the parameters of magnetic field H and f_1 (the limit frequency) resulting from the condition given by Equation (13).

No.	H (kA/m)	f_1 (kHz)	D_o (nm)	$(P_{sM})_l$ (W/g)
1	5	1000	5.88	2.69 (+0.48)
2	15	334	6.25	9.73 (+0.43)
3	30	167	6.46	21.26 (+0.15)
4	45	111	6.58	32.70 (+0.02)
5	60	83	6.67	43.36 (+0.07)
6	75	67	6.72	53.43 (−0.30)
7	90	56	6.77	62.04 (−0.40)
8	100	50	6.80	66.46 (+0.14)
9	120	42	6.84	75.19 (−0.31)
10	135	37	6.88	79.50 (+0.27)
11	150	33	6.91	82.87 (+0.80)
12	165	30	6.93	86.27 (+0.47)
13	180	28	6.95	89.99 (−0.89)

The dependence of the maximum specific loss power ($(P_{sM})_l$) in the admissible biological limit (Equation (13)) as a function of the amplitude of magnetic field (H) is shown in Figure 8. The mean values of the function ($(P_{sM})_l$) are shown in figure by the red fit curve, and the predict limits interval is shown by the light blue color.

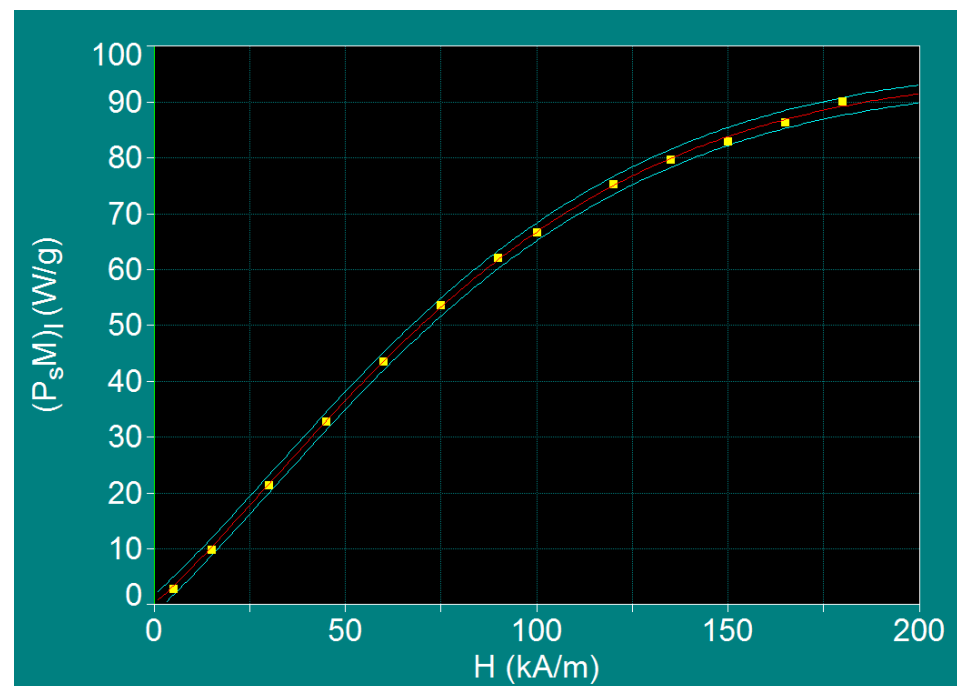


Figure 8. The variation of maximum specific loss power within the admissible biological limits ($(P_{sM})_l$) as a function of the magnetic field H in the case of CoFe_2O_4 nanoparticles.

While analyzing this dependence, it was observed that, in the case of CoFe_2O_4 nanoparticles, the maximum specific loss power ($(P_{sM})_l$) increases proportionally with the increase of the magnetic field up to 90–100 kA/m. Above these values, the maximum specific loss power tends towards saturation.

Therefore, exploring different values for the magnetic field higher than 100 kA/m is not recommended for practical use, at least for two reasons: (i) the power gain is reduced more and more as the field increases, decreasing its efficiency, and (ii) obtaining large magnetic fields at frequencies in the order of hundreds of kHz is difficult to achieve in

practice. In addition, considering the results from Section 3.3.2 and even Section 3.3.1, we recommend the use of a magnetic field up to the maximum limit of 60 kA/m, respectively in the range 5–60 kA/m. This is the optimal range, shown by the green color in Table 3, which can be used with maximum efficiency in the case of superparamagnetic hyperthermia with CoFe₂O₄ ferrimagnetic nanoparticles. The optimal values corresponding to the diameter of the magnetic nanoparticles D_{op} and the limit frequency of the magnetic field f_1 are given in Table 3.

Comparing these results with those obtained in the case of magnetite nanoparticles [53], having 10–25 kA/m for the amplitude of the magnetic field and 200–500 kHz for the frequency, we find that in the case of CoFe₂O₄ nanoparticles we've achieved a much wider range for both the magnetic field and frequency, respectively 5–60 kA/m and 83–1000 kHz. This is of great practical advantage, as having a very wide range of values for the magnetic field and frequency in which superparamagnetic hyperthermia can be efficiently obtained for nanoparticles with sizes in the range 5.88–6.67 nm.

Such a major advantage of the CoFe₂O₄ nanoparticles together with obtaining intracellular hyperthermia due to the very small sizes of these nanoparticles can make the superparamagnetic hyperthermia with CoFe₂O₄ ferrite nanoparticles more versatile than the one with Fe₃O₄ nanoparticles, although the latter has been mostly used so far in cancer therapy.

However, under these conditions, there's still another matter that should be verified in order to be able to support without a doubt the versatility of the superparamagnetic hyperthermia with CoFe₂O₄ nanoparticles, namely, if the power is significantly lower in the case of CoFe₂O₄ nanoparticles compared to that obtained for Fe₃O₄ nanoparticles would be sufficient to heat CoFe₂O₄ nanoparticles to the optimum temperature of 43 °C used in hyperthermia for the effective destruction of tumor cells. This issue is presented and discussed in the next section.

3.5. Heating Characteristics and Optimum Heating Time in the Case of Superparamagnetic Hyperthermia with CoFe₂O₄ Nanoparticles

Using Equation (8) where the specific loss power P_s is given by Equation (2) or (7) depending on the magnetic field used (as we have shown above), with the quantities ξ , χ_i and τ given by Equations (3), (5) and (6), we calculated the variation of the heating temperature (ΔT_h) of the CoFe₂O₄ nanoparticles and the heating time (Δt_o) to reach the optimal heating temperature (T_o) of ~43 °C required in magnetic hyperthermia of cancer. In the calculations we took into account the room temperature (T_r) of 25 °C as the initial temperature at which the nanoparticles are found. In order to reach the optimum temperature (T_o) of 43 °C it would be necessary to increase the heating temperature (ΔT_{ho}) by 18 °C compared to the room temperature ($T_o = T_r + \Delta T_{ho}$). At the same time, we took into account in the calculations the dependence of the parameters in Equations (3), (5) and (6) on the temperature increase above the room temperature. Thus, we calculated the variation (increase) of the heating temperature ΔT_h starting from the room temperature T_r (25 °C). This increase must be at least 18 °C in order to reach the optimum temperature T_o of 43 °C.

The results obtained for the magnetic field of 5 kA/m and 60 kA/m (the limits of the optimal range) in optimal conditions, and within the admissible biological limit (according to the values in Table 3) are shown in Figure 9. The results show that in both cases a ΔT_h increase of the temperature is obtained by more than 18 °C above the room temperature (25 °C), thus reaching the optimal temperature of 43 °C for both values of the magnetic field.

For example, in the case of the magnetic field of 5 kA/m (Figure 9a) the temperature ΔT_{ho} increased by 18 °C more than the room temperature and takes place in the Δt_o time interval of 5.01 s. The maximum heating temperature variation (ΔT_{hm}) of 42.43 °C is reached after time interval Δt_m of 23.63 s. However, if the magnetic field has a high value of 60 kA/m (Figure 9b) the temperature variation of 18 °C is obtained faster, in a shorter period of time (Δt_o) of only 0.35 s, and the maximum heating temperature (ΔT_{hm}) in this case is lower, being 26.74 °C compared to 42.43 °C as in the previous case, a value that is reached in a period of time (Δt_m) of only 0.92 s.

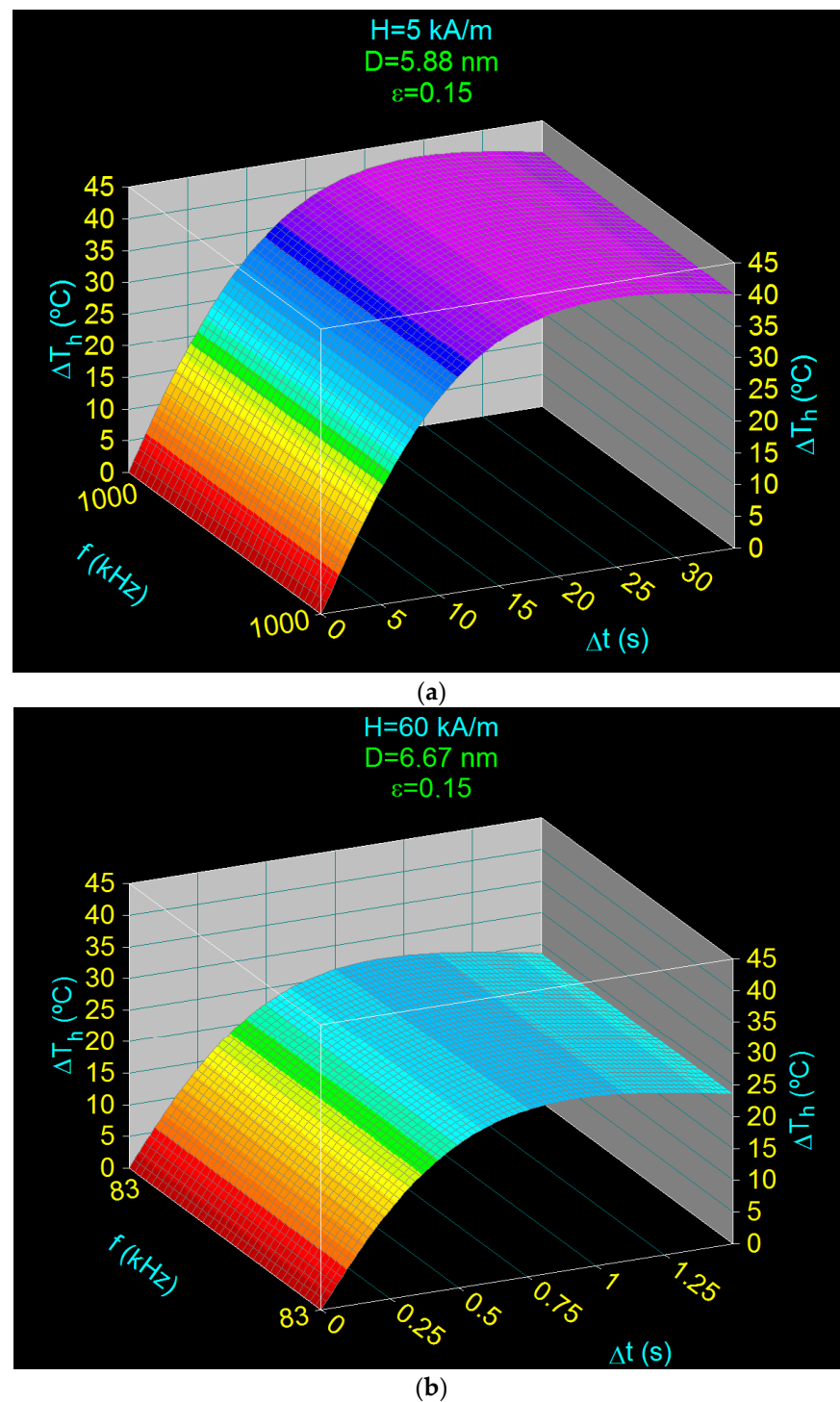


Figure 9. The time variation of heating temperature (ΔT_h) of CoFe_2O_4 nanoparticles in optimal conditions given in Table 3 for volume fraction of 0.15 and two values of magnetic field: (a) 5 kA/m and (b) 60 kA/m.

Thus, when the magnetic field increases to 60 kA/m a significant reduction in the heating time of the nanoparticles is obtained, approx. 14 times lower, which is greatly advantageous in terms of the hyperthermic effect (heating must be done in the shortest possible time so as not to affect healthy cells). However, in this case, there is also a decrease in the maximum temperature reached, from 42.43 °C to 26.74 °C, mainly due to the decrease in the frequency limit from 1000 kHz to 83 kHz used in this case. However, this does not

affect the hyperthermic effect, increasing the temperature by 18 °C above room temperature being achieved, and the optimal temperature of 43 °C being obtained.

Using 3D representations such as those in Figure 9 for the optimal conditions in Table 3 (field values in the range 5–60 kA/m, limit frequencies in the range 83–1000 kHz and the optimal diameter of nanoparticles in the range 5.88–6.67 nm) we determined all values for the optimal time intervals (Δt_o) (marked in green) necessary to reach the optimum temperature of 43 °C (increase with $\Delta T_{ho} = 18$ °C above room temperature), as well as the values of the maximum temperature ΔT_{hm} that is reached and the times Δt_m required for this. The values obtained are shown in Table 4.

Table 4. The values of the optimal heating times (Δt_o) of the CoFe₂O₄ nanoparticles under the optimal parameters given in Table 3, for the volume fraction of 0.15. The table also shows the values of the maximum variation of the heating temperature (ΔT_{hm}) of the nanoparticles and their corresponding durations (Δt_m) under the given conditions.

H (kA/m)	f _l (kHz)	D _o (nm)	ΔT_{hm} (°C)	Δt_m (s)	* ΔT_{ho} (°C)	** Δt_o (s)
5	1000	5.88	42.43	23.33	18	5.01
15	334	6.25	33.35	5.18	18	1.45
30	167	6.46	29.29	2.09	18	0.69
45	111	6.58	27.48	1.27	18	0.46
60	83	6.67	26.74	0.92	18	0.35

* $\Delta T_{ho} = 43-25$ °C; ** (± 0.01).

However, considering that in practice smaller packing fractions can be used, in order to check the heating efficiency in these cases we also considered another much smaller fraction, namely $\epsilon = 0.017$. The results obtained in this case are shown in Figure 10 for the same magnetic fields as in the previous case: 5 kA/m (Figure 10a) and 60 kA/m (Figure 10b).

The results show that even in these cases the optimal heating of CoFe₂O₄ nanoparticles can be obtained at the optimum temperature (T_o) of 43 °C, only that this will be done in a longer time interval (Δt_o). For example, in the case of a magnetic field of 5 kA/m (Figure 10a), a heating of the nanoparticles by 18 °C in addition to the room temperature (25 °C) in order to reach the optimal value of 43 °C, will be made in a time interval (optimal) Δt_o of ~44 s compared to only ~5 s in the previous case.

The optimal values for the time intervals (Δt_o) determined in this case for different values of the magnetic field in the range of 5–60 kA/m, in the optimal conditions and in the biologically admissible limits, are given in Table 5. From the table it is observed that increasing the amplitude of the applied magnetic field leads to a decrease in the heating time, as we expected.

Table 5. The values of the optimal heating times (Δt_o) of the CoFe₂O₄ nanoparticles under the optimal parameters given in Table 3, for the volume fraction of 0.017. The table also shows the values of the maximum variation of the heating temperature (ΔT_{hm}) of the nanoparticles and their corresponding durations (Δt_m) under the given conditions.

H (kA/m)	f _l (kHz)	D _o (nm)	ΔT_{hm} (°C)	Δt_m (s)	* ΔT_{ho} (°C)	** Δt_o (s)
5	1000	5.88	41.99	212.07	18	44.19
15	334	6.25	33.06	46.57	18	12.80
30	167	6.46	28.81	18.15	18	6.14
45	111	6.58	27.28	11.15	18	4.08
60	83	6.67	26.72	8.08	18	3.07

* $\Delta T_{ho} = 43-25$ °C; ** (± 0.01).

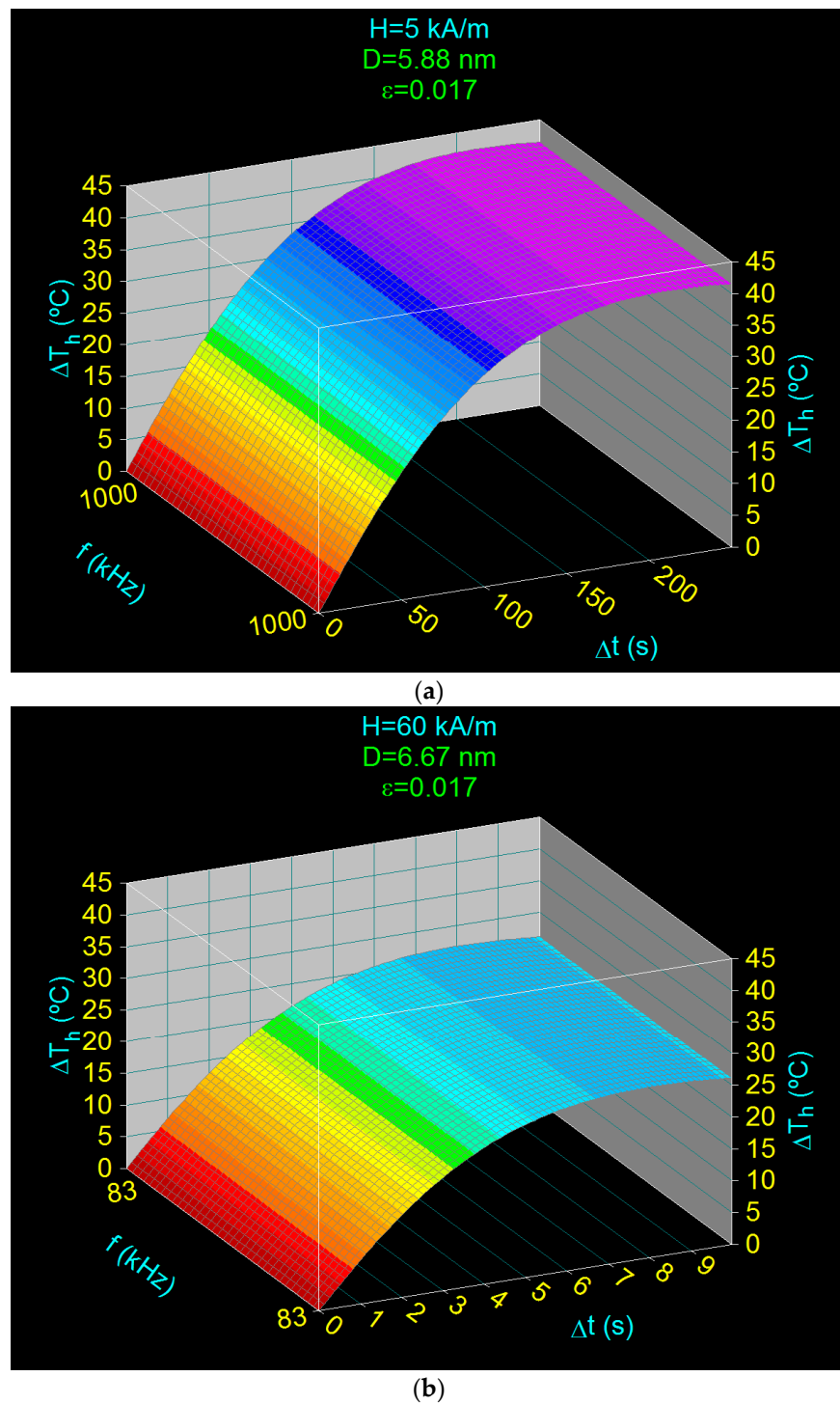


Figure 10. The time variation of heating temperature (ΔT_h) of CoFe_2O_4 nanoparticles in optimal conditions given in Table 3 for volume fraction of 0.017 and two values of magnetic field: (a) 5 kA/m and (b) 60 kA/m.

Considering all the above results obtained for both ϵ of 0.017 and 0.15 we can say that for all other values of ϵ in the range 0.017–0.15 the optimal heating of the nanoparticles at temperatures of 43 °C will be possible. The optimal heating times (Δt_0) will be found between the two limits given in Tables 4 and 5, for each value of the magnetic field. For example, in the case of the applied magnetic field of 5 kA/m the optimal heating times of the nanoparticles in order to reach the effective temperature of 43 °C will be in the range of 5.01–44.19 s, depending on the value of the volume fraction (ϵ).

Also, according to the data in Tables 4 and 5, it results that the optimal heating times of CoFe_2O_4 nanoparticles are quite short in all cases, being fulfilled the condition of magnetic hyperthermia not to affect healthy cells.

In conclusion, according to the results obtained, we can say that in all cases considered for the optimally established range (Table 3, values marked in green) an efficient heating of CoFe_2O_4 nanoparticles will be obtained, and, therefore, these can be successfully used in superparamagnetic hyperthermia. Even if the maximum specific loss power $(P_{SM})_1$ within the admissible biological limit in the case of CoFe_2O_4 nanoparticles is significantly lower (Table 3) than in the case of magnetite nanoparticles [28,53], still CoFe_2O_4 nanoparticles can be used successfully in superparamagnetic hyperthermia, because under the optimal conditions established by us the nanoparticles can be heated to the optimum temperature of 43°C necessary in magnetic hyperthermia for the effective destruction of tumor cells. Thus, the issue of efficient heating of CoFe_2O_4 nanoparticles under conditions of low specific loss power (point (iv) of Section 3.2) has also been clarified.

4. Conclusions

In this paper we have demonstrated that small nanoparticles (5.88–6.67 nm) of CoFe_2O_4 ferrite can be successfully used in superparamagnetic hyperthermia for alternative cancer therapy, under the following optimal conditions for practical implementation:

- (1) Obtaining the heating temperature of the nanoparticles at 43°C for the amplitudes of the magnetic field of 5–60 kA/m, the frequencies of the magnetic field of 83–1000 kHz, and the diameters of the nanoparticles in the range 5.88–6.67 nm (Sections 3.4 and 3.5);
- (2) Optimal heating of the nanoparticles, by 18°C above room temperature (25°C), in a short period of time: 0.35–44.19 s, depending on the volume packing fractions;
- (3) The use of the linear approximation up to large magnetic fields, of ~ 60 –70 kA/m, for the maximum specific loss power, which greatly simplifies the practical implementation of magnetic hyperthermia in the case of CoFe_2O_4 nanoparticles.
- (4) Possible intracellular therapy due to the use of very small nanoparticles (5.88–6.67 nm) of CoFe_2O_4 that lead to obtaining the optimal maximum specific loss power (P_{sMo}) , a therapy that is much more effective in destroying tumor cells.

All optimal values of the amplitude (H) and frequency (f) of the magnetic field, the optimal nanoparticle diameter (D_o) and the optimal heating times (Δt_o) are given in Table 3 (values marked in green), and the graphic in Figure 8. The corresponding optimal times are found in Tables 4 and 5, as well as Figures 9 and 10.

These all results, under the appropriate biocompatible of CoFe_2O_4 nanoparticles with the biological tissue into which they are to be inserted, may make CoFe_2O_4 nanoparticles more effective than magnetite (Fe_3O_4) in cancer therapy by superparamagnetic hyperthermia.

Also, the possible use of magnetic fields in a very wide range of values for its amplitude and frequency (5–60 kA/m and 83–1000 kHz) in the case of superparamagnetic hyperthermia with CoFe_2O_4 ferrite nanoparticles is another major practical advantage. This will lead to eliminating the restrictive conditions in relation to the magnetic field used so far in the case of magnetite (10–25 kA/m and 200–500 kHz [53]).

In addition, for greater accuracy in the practical application of magnetic hyperthermia, it is recommended to determine experimentally a priori the effective magnetic anisotropy and the spontaneous/saturation magnetization of nanoparticles to be used, give the possible surface effects in nanoparticles which could contribute to the modification of these parameters.

All these will allow in practice to adjust on a case-by-case basis, the values used for magnetic field parameters and nanoparticle sizes to obtain the maximum effect in superparamagnetic hyperthermia for each particular tissue for maximum efficacy in destroying tumor cells.

Funding: This work was supported by a grant of the Ministry of Research, Innovation and Digitization, CNCS/CCCDI—UEFISCDI, project number PN-III-P2-2.1-PED-2019-3067 (contract no. 263PED/2020), within PNCDI III.

Institutional Review Board Statement: Not applicable.

Informed Consent Statement: Not applicable.

Data Availability Statement: This is not applicable.

Conflicts of Interest: The author declares no conflict of interest.

References

1. Rosensweig, R. Heating magnetic fluid with alternating magnetic field. *J. Magn. Magn. Mater.* **2002**, *252*, 370–374. [[CrossRef](#)]
2. Néel, L. Théorie du traînage magnétique des ferromagnétiques en grains fins avec application aux terres cuites. *Ann. Geophys.* **1949**, *5*, 99–136.
3. Bean, C.P.; Livingston, L.D. Superparamagnetism. *J. Appl. Phys.* **1959**, *30*, S120–S129. [[CrossRef](#)]
4. Caizer, C. Magnetic behavior of $Mn_{0.6}Fe_{0.4}Fe_2O_4$ nanoparticles in ferrofluid at low temperatures. *J. Magn. Magn. Mater.* **2002**, *251*, 304. [[CrossRef](#)]
5. Perigo, E.A.; Hemery, G.; Sandre, O.; Ortega, D.; Garaio, E.; Plazaola, F.; Teran, F.J. Fundamentals and advances in magnetic hyperthermia. *Appl. Phys. Rev.* **2015**, *2*, 41302. [[CrossRef](#)]
6. Caizer, C. Nanoparticle size effect on some magnetic properties. In *Handbook of Nanoparticles*; Aliofkhaezrai, M., Ed.; Springer: Cham, Switzerland, 2016; pp. 475–519.
7. Caizer, C. Magnetic hyperthermia-using magnetic metal/oxide nanoparticles with potential in cancer therapy. In *Metal Nanoparticles in Pharma*; Rai, M., Shegokar, R., Eds.; Springer: Cham, Switzerland, 2017; pp. 193–218.
8. Brown, W.F., Jr. Thermal fluctuations of a single-domain particle. *Phys. Rev.* **1963**, *130*, 1677–1686. [[CrossRef](#)]
9. Torres, T.E.; Lima, E., Jr.; Calatayud, M.P.; Sanz, B.; Ibarra, A.; Fernández-Pacheco, R.; Mayoral, A.; Marquina, C.; Ibarra, M.R.; Goya, G.F. The relevance of brownian relaxation as power absorption mechanism in magnetic hyperthermia. *Sci. Rep.* **2019**, *9*, 3992. [[CrossRef](#)] [[PubMed](#)]
10. Caizer, C. Magnetic/Superparamagnetic hyperthermia as an effective noninvasive alternative method for therapy of malignant tumors. In *Nanotheranostics: Applications and Limitations*; Rai, M., Jamil, B., Eds.; Springer: Cham, Switzerland, 2019; pp. 297–335.
11. Caizer, C. Magnetic/Superparamagnetic hyperthermia in clinical trials for noninvasive alternative cancer therapy. In *Magnetic Nanoparticles in Human Health and Medicine: Current Medical Applications and Alternative Therapy of Cancer*; Caizer, C., Rai, M., Eds.; Wiley: Oxford, UK, 2021. (In Press)
12. Caizer, C.; Rai, M. Magnetic nanoparticles in alternative tumors therapy: Biocompatibility, toxicity and safety compared with classical methods. In *Magnetic Nanoparticles in Human Health and Medicine: Current Medical Applications and Alternative Therapy of Cancer*; Caizer, C., Rai, M., Eds.; Wiley: Oxford, UK, 2021. (In Press)
13. Ito, A.; Tanaka, K.; Honda, H.; Abe, S.; Yamaguchi, H.; Kobayashi, T. Complete regression of mouse mammary carcinoma with a size greater than 15 mm by frequent repeated hyperthermia using magnetite nanoparticles. *J. Biosci. Bioeng.* **2003**, *96*, 364–369. [[CrossRef](#)]
14. Hilger, I.; Hergt, R.; Kaiser, W.A. Towards breast cancer treatment by magnetic heating. *J. Magn. Magn. Mater.* **2005**, *293*, 314–319. [[CrossRef](#)]
15. Tanaka, K.; Ito, A.; Kobayashi, T.; Kawamura, T.; Shimada, S.; Matsumoto, K.; Saida, T.; Honda, H. Intratumoral injection of immature dendritic cells enhances antitumor effect of hyperthermia using magnetic nanoparticles. *Int. J. Cancer* **2005**, *116*, 624–633. [[CrossRef](#)]
16. Johannsen, M.; Thiesen, B.; Jordan, A.; Taymoorian, K.; Gneveckow, U.; Waldöfner, N.; Scholz, R.; Koch, M.; Lein, M.; Jung, K.; et al. Magnetic fluid hyperthermia (MFH) reduces prostate cancer growth in the orthotopic Dunning R3327 rat model. *Prostate* **2005**, *64*, 283–292. [[CrossRef](#)]
17. Jordan, A.; Scholz, R.; Maier-Hauff, K.; van Landeghem, F.; Waldöfner, N.; Teichgraber, U.; Pinkernelle, J.; Bruhn, H.; Neumann, F.; Thiesen, B.; et al. The effect of thermotherapy using magnetic nanoparticles on rat malignant glioma. *J. NeuroOncol.* **2006**, *78*, 7–14. [[CrossRef](#)]
18. Maier-Hauff, K.; Rothe, R.; Scholz, R.; Gneveckow, U.; Wust, P.; Thiesen, B.; Feussner, A.; von Deimling, A.; Waldöfner, N.; Felix, R.; et al. Intracranial Thermotherapy using Magnetic Nanoparticles Combined with External Beam Radiotherapy: Results of a Feasibility Study on Patients with Glioblastoma Multiforme. *J. NeuroOncol.* **2007**, *81*, 53–60. [[CrossRef](#)]
19. Gazeau, F.; Levy, M.; Wilhelm, C. Optimizing magnetic nanoparticle design for nanothermotherapy. *Nanomedicine* **2008**, *3*, 831–844. [[CrossRef](#)]
20. Hou, C.-H.; Hou, S.-M.; Hsueh, Y.-S.; Lin, J.; Wu, H.-C.; Lin, F.-H. The in vivo performance of biomagnetic hydroxyapatite nanoparticles in cancer hyperthermia therapy. *Biomaterials* **2009**, *30*, 3956–3960. [[CrossRef](#)] [[PubMed](#)]
21. Kobayashi, T. Cancer hyperthermia using magnetic nanoparticles. *Biotechnol. J.* **2011**, *6*, 1342–1347. [[CrossRef](#)]
22. Alphandéry, E.; Chebbi, I.; Guyot, F.; Durand-Dubief, M. Use of bacterial magnetosomes in the magnetic hyperthermia treatment of tumours: A review. *Int. J. Hyperth.* **2013**, *29*, 801–809. [[CrossRef](#)] [[PubMed](#)]

23. Hilger, I. In vivo applications of magnetic nanoparticle Hyperthermia. *Int. J. Hypertherm.* **2013**, *29*, 828–834. [CrossRef] [PubMed]
24. Espinosa, A.; Bugnet, M.; Radtke, G.; Neveu, S.; Botton, G.A.; Wilhelm, C.; Abou-Hassan, A. Can magneto-plasmonic nanohybrids efficiently combine photothermia with magnetic hyperthermia? *Nanoscale* **2015**, *7*, 18872–18877. [CrossRef]
25. Wang, P.; Xie, X.; Wang, J.; Shi, Y.; Shen, N.; Huang, X. Ultra-small superparamagnetic iron oxide mediated magnetic hyperthermia in treatment of neck lymph node metastasis in rabbit pyriform sinus VX2 carcinoma. *Tumor Biol.* **2015**, *36*, 8035–8040. [CrossRef]
26. Alphanđéry, E.; Idbaih, A.; Adam, C.; Delattre, J.-Y.; Schmitt, C.; Guyot, F.; Chebbi, I. Chains of magnetosomes with controlled endotoxin release and partial tumor occupation induce full destruction of intracranial U87-Luc glioma in mice under the application of an alternating magnetic field. *J. Control. Release* **2017**, *262*, 259–272. [CrossRef]
27. Gupta, R.; Sharma, D. Evolution of Magnetic Hyperthermia for Glioblastoma Multiforme Therapy. *ACS Chem. Neurosci.* **2019**, *10*, 1157–1172. [CrossRef] [PubMed]
28. The NanoTherm® Therapy, MagForce Nanomedicine, Germany. Available online: https://www.magforce.com/en/home/our_therapy/ (accessed on 28 April 2021).
29. Kikumori, T.; Kobayashi, T.; Sawaki, M.; Imai, T. Anti-cancer effect of hyperthermia on breast cancer by magnetite nanoparticle-loaded anti-HER2 immunoliposomes. *Breast Cancer Res. Treat.* **2009**, *113*, 435–441. [CrossRef] [PubMed]
30. Laurent, S.; Dutz, S.; Häfeli, U.O.; Mahmoudi, M. Magnetic fluid hyperthermia: Focus on superparamagnetic iron oxide nanoparticles. *Adv. Colloid Interface Sci.* **2011**, *166*, 8–23. [CrossRef]
31. Caizer, C. Computational study on superparamagnetic hyperthermia with biocompatible SPIONs to destroy the cancer cells. *J. Phys. Conf. Ser.* **2014**, *521*, 12015. [CrossRef]
32. Di Corato, R.; Béalle, G.; Kolosnjaj-Tabi, J.; Espinosa, A.; Clément, O.; Silva, A.; Ménager, C.; Wilhelm, C. Combining magnetic hyperthermia and photodynamic therapy for tumor ablation with photoresponsive magnetic liposomes. *ACS Nano* **2015**, *9*, 2904–2916. [CrossRef]
33. Wang, F.; Yang, Y.; Ling, Y.; Liu, J.; Cai, X.; Zhou, X.; Tang, X.; Liang, B.; Chen, Y.; Chen, H.; et al. Injectable and thermally contractible hydroxypropyl methyl cellulose/Fe₃O₄ for magnetic hyperthermia ablation of tumors. *Biomaterials* **2017**, *128*, 84–93. [CrossRef]
34. Yan, H.; Shang, W.; Sun, X.; Zhao, L.; Wang, J.; Xiong, Z.; Yuan, J.; Zhang, R.; Huang, Q.; Wang, K.; et al. “All-in-One” Nanoparticles for Trimodality Imaging-Guided Intracellular Photo-magnetic Hyperthermia Therapy under Intravenous Administration. *Adv. Funct. Mater.* **2018**, *28*. [CrossRef]
35. Kandasamy, G.; Sudame, A.; Bhati, P.; Chakrabarty, A.; Maity, D. Systematic investigations on heating effects of carboxyl-amine functionalized superparamagnetic iron oxide nanoparticles (SPIONs) based ferrofluids for in vitro cancer hyperthermia therapy. *J. Mol. Liq.* **2018**, *256*, 224–237. [CrossRef]
36. Mondal, S.; Manivasagan, P.; Bharathiraja, S.; Moorthy, M.S.; Nguyen, V.T.; Kim, H.H.; Nam, S.Y.; Lee, K.D.; Oh, J. Hydroxyapatite Coated Iron Oxide Nanoparticles: A Promising Nanomaterial for Magnetic Hyperthermia Cancer Treatment. *Nanomaterials* **2017**, *7*, 426. [CrossRef]
37. Xu, H.; Pan, Y. Experimental evaluation on the heating efficiency of magnetoferritin nanoparticles in an alternating magnetic field. *Nanomaterials* **2019**, *9*, 1457. [CrossRef]
38. Zhao, S.; Lee, S. Biomaterial-modified magnetic nanoparticles γ -Fe₂O₃, Fe₃O₄ used to improve the efficiency of hyperthermia of tumors in HepG2 model. *Appl. Sci.* **2021**, *11*, 2017. [CrossRef]
39. Narayanaswamy, V.; Sambasivam, S.; Saj, A.; Alaabed, S.; Issa, B.; Al-Omari, I.A.; Obaidat, I.M. Role of magnetite nanoparticles size and concentration on hyperthermia under various field frequencies and stren. *Molecules* **2021**, *26*, 796. [CrossRef]
40. Pradhan, P.; Giri, J.; Samanta, G.; Sarma, H.D.; Mishra, K.P.; Bellare, J.; Banerjee, R.; Bahadur, D. Comparative evaluation of heating ability and biocompatibility of different ferrite-based magnetic fluids for hyperthermia application. *J. Biomed. Mater. Res. Part B Appl. Biomater.* **2007**, *81*, 12–22. [CrossRef]
41. Prasad, N.K.; Rathinasamy, K.; Panda, D.; Bahadur, D. Mechanism of cell death induced by magnetic hyperthermia with nanoparticles of γ -MnxFe_{2-x}O₃ synthesized by a single step process. *J. Mat. Chem.* **2007**, *17*, 5042–5051. [CrossRef]
42. Hejase, H.; Hayek, S.S.; Qadri, S.; Haik, Y. MnZnFe nanoparticles for self-controlled magnetic hyperthermia. *J. Magn. Magn. Mater.* **2012**, *324*, 3620–3628. [CrossRef]
43. Qu, Y.; Li, J.; Ren, J.; Leng, J.; Lin, C.; Shi, D. Enhanced Magnetic Fluid Hyperthermia by Micellar Magnetic Nanoclusters Composed of MnxZn_{1-x}Fe₂O₄ Nanoparticles for Induced Tumor Cell Apoptosis. *ACS Appl. Mater. Interfaces* **2014**, *6*, 16867–16879. [CrossRef] [PubMed]
44. Saldívar-Ramírez, M.M.G.; Sánchez-Torres, C.G.; Cortés-Hernández, D.A.; Escobedo-Bocardo, J.C.; Almanza, J.; Larson, A.; Reséndiz-Hernández, P.J.; Acuña-Gutiérrez, I.O. Study on the efficiency of nanosized magnetite and mixed ferrites in magnetic hyperthermia. *J. Mater. Sci. Mater. Electron.* **2014**, *25*, 2229–2236. [CrossRef]
45. Almaki, J.H.; Nasiri, R.; Idris, A.; Majid, F.A.A.; Salouti, M.; Wong, T.S.; Dabagh, S.; Marvibaigi, M.; Amini, N. Synthesis, characterization and in vitro evaluation of exquisite targeting SPIONs-PEG-HER in HER2+ human breast cancer cells. *Nanotechnology* **2016**, *27*, 105601. [CrossRef] [PubMed]
46. Liu, X.L.; Ng, C.T.; Chandrasekharan, P.; Yang, H.T.; Zhao, L.Y.; Peng, E.; Lv, Y.B.; Xiao, W.; Fang, J.; Yi, J.B.; et al. Synthesis of ferromagnetic Fe_{0.6}Mn_{0.4}O nanoflowers as a new class of magnetic theranostic platform for in vivo T1-T2 dual-mode magnetic resonance imaging and magnetic hyperthermia therapy. *Adv. Healthc. Mater.* **2016**, *5*, 2092–2104. [CrossRef] [PubMed]

47. Wu, W.; Wu, Z.; Yu, T.; Jiang, C.; Kim, W.-S. Recent progress on magnetic iron oxide nanoparticles: Synthesis, surface functional strategies and biomedical applications. *Sci. Technol. Adv. Mater.* **2015**, *16*, 23501. [[CrossRef](#)] [[PubMed](#)]
48. Martín-Saavedra, F.; Ruíz-Hernández, E.; Boré, A.; Arcos, D.; Vallet-Regí, M.; Vilaboa, N. Magnetic mesoporous silica spheres for hyperthermia therapy. *Acta Biomater.* **2010**, *6*, 4522–4531. [[CrossRef](#)]
49. Meneses-Brassea, B.P.; Borrego, E.A.; Blazer, D.S.; Sanad, M.F.; Pourmiri, S.; Gutierrez, D.A.; Varela-Ramirez, A.; Hadjipanayis, G.C.; El-Gendy, A.A. Ni-Cu Nanoparticles and Their Feasibility for Magnetic Hyperthermia. *Nanomaterials* **2020**, *10*, 1988. [[CrossRef](#)] [[PubMed](#)]
50. Reyes-Ortega, F.; Delgado, Á.; Iglesias, G. Modulation of the Magnetic Hyperthermia Response Using Different Superparamagnetic Iron Oxide Nanoparticle Morphologies. *Nanomaterials* **2021**, *11*, 627. [[CrossRef](#)]
51. Albarqi, H.A.; Demessie, A.A.; Sabei, F.Y.; Moses, A.S.; Hansen, M.N.; Dhagat, P.; Taratula, O.R.; Taratula, O. Systemically Delivered Magnetic Hyperthermia for Prostate Cancer Treatment. *Pharmaceutics* **2020**, *12*, 1020. [[CrossRef](#)]
52. Purushotham, S.; Ramanujan, R.V. Modeling the performance of magnetic nanoparticles in multimodal cancer therapy. *J. Appl. Phys.* **2010**, *107*, 114701. [[CrossRef](#)]
53. Caizer, C. Optimization Study on Specific Loss Power in Superparamagnetic Hyperthermia with Magnetite Nanoparticles for High Efficiency in Alternative Cancer Therapy. *Nanomaterials* **2020**, *11*, 40. [[CrossRef](#)]
54. Smit, J.; Wijn, H.P.J. *Les Ferites*; Bibliothèque Technique Philips: Paris, France, 1961.
55. Valenzuela, R. *Magnetic Ceramics*; Cambridge University Press: Cambridge, UK, 1994.
56. Fortin, J.-P.; Gazeau, F.; Wilhelm, C. Intracellular heating of living cells through Néel relaxation of magnetic nanoparticles. *Eur. Biophys. J.* **2008**, *37*, 223–228. [[CrossRef](#)] [[PubMed](#)]
57. Balakrishnan, P.B.; Silvestri, N.; Fernandez-Cabada, T.; Marinaro, F.; Fernandes, S.; Fiorito, S.; Miscuglio, M.; Serantes, D.; Ruta, S.; Livesey, K.; et al. Exploiting Unique Alignment of Cobalt Ferrite Nanoparticles, Mild Hyperthermia, and Controlled Intrinsic Cobalt Toxicity for Cancer Therapy. *Adv. Mater.* **2020**, *32*, e2003712. [[CrossRef](#)] [[PubMed](#)]
58. Kharat, P.B.; Somvanshi, S.B.; Khirade, P.P.; Jadhav, K.M. Induction Heating Analysis of Surface-Functionalized Nanoscale CoFe₂O₄ for Magnetic Fluid Hyperthermia toward Noninvasive Cancer Treatment. *ACS Omega* **2020**, *5*, 23378–23384. [[CrossRef](#)] [[PubMed](#)]
59. Dutz, S.; Buske, N.; Landers, J.; Gräfe, C.; Wende, H.; Clement, J.H. Biocompatible Magnetic Fluids of Co-Doped Iron Oxide Nanoparticles with Tunable Magnetic Properties. *Nanomaterials* **2020**, *10*, 1019. [[CrossRef](#)]
60. Khizar, S.; Ahmad, N.; Ahmed, N.; Manzoor, S.; Hamayun, M.; Naseer, N.; Tenório, M.; Lebaz, N.; Elaissari, A. Aminodextran coated CoFe₂O₄ nanoparticles for combined magnetic resonance imaging and hyperthermia. *Nanomaterials* **2020**, *10*, 2182. [[CrossRef](#)]
61. Medina, M.A.; Oza, G.; Ángeles-Pascual, A.; González, M.M.; Antaño-López, R.; Vera, A.; Leija, L.; Reguera, E.; Arriaga, L.G.; Hernández, J.M.H.; et al. Synthesis, Characterization and Magnetic Hyperthermia of Monodispersed Cobalt Ferrite Nanoparticles for Cancer Therapeutics. *Molecules* **2020**, *25*, 4428. [[CrossRef](#)] [[PubMed](#)]
62. Das, R.; Kim, N.P.; Attanayake, S.; Phan, M.-H.; Srikanth, H. Role of magnetic anisotropy on the hyperthermia efficiency in spherical Fe_{3-x}Co_xO₄ (x = 0 – 1) nanoparticles. *Appl. Sci.* **2021**, *11*, 930. [[CrossRef](#)]
63. Lucht, N.; Friedrich, R.P.; Draack, S.; Alexiou, C.; Viereck, T.; Ludwig, F.; Hankiewicz, B. Biophysical Characterization of (Silica-coated) Cobalt Ferrite Nanoparticles for Hyperthermia Treatment. *Nanomaterials* **2019**, *9*, 1713. [[CrossRef](#)]
64. Verde, E.L.; Landi, G.T.; Gomes, J.D.A.; Sousa, M.H.; Bakuzis, A.F. Magnetic hyperthermia investigation of cobalt ferrite nanoparticles: Comparison between experiment, linear response theory, and dynamic hysteresis simulations. *J. Appl. Phys.* **2012**, *111*, 123902. [[CrossRef](#)]
65. Mohapatra, J.; Xing, M.; Liu, J.P. Magnetic and hyperthermia properties of CoxFe_{3-x}O₄ nanoparticles synthesized via cation exchange. *AIP Adv.* **2018**, *8*, 56725. [[CrossRef](#)]
66. Leonel, A.G.; Mansur, A.A.P.; Carvalho, S.M.; Outon, L.E.F.; Ardisson, J.D.; Krambrock, K.; Mansur, H.S. Tunable magnetothermal properties of cobalt-doped magnetite–carboxymethylcellulose ferrofluids: Smart nanoplatforms for potential magnetic hyperthermia applications in cancer therapy. *Nanoscale Adv.* **2021**, *3*, 1029–1046. [[CrossRef](#)]
67. Habib, A.H.; Ondeck, C.L.; Chaudhary, P.; Bockstaller, M.R.; McHenry, M.E. Evaluation of iron-cobalt/ferrite core-shell nanoparticles for cancer thermotherapy. *J. Appl. Phys.* **2008**, *103*. [[CrossRef](#)]
68. Langevin, P. Magnétisme et théorie des électrons. *Ann. Chem. Phys.* **1905**, *5*, 70–127.
69. Jacobs, I.S.; Bean, C.P. Fine particles, thin films and exchange anisotropy. In *Magnetism*; Rado, G.T., Suhl, H., Eds.; Academic Press: Cambridge, MA, USA, 1963; Volume 3, pp. 271–350.
70. Back, C.; Weller, D.; Heidmann, J.; Mauri, D.; Guarisco, D.; Garwin, E.L.; Siegmann, H.C. Magnetization Reversal in Ultrashort Magnetic Field Pulses. *Phys. Rev. Lett.* **1998**, *81*, 3251–3254. [[CrossRef](#)]
71. Coey, J.M.D. Noncollinear spin arrangement in ultrafine ferrimagnetic crystallites. *Phys. Rev. Lett.* **1971**, *27*, 1140. [[CrossRef](#)]
72. Kodama, R.H.; Berkowitz, A.E.; McNiff, E.J., Jr.; Foner, S. Surface spin disorder in NiFe₂O₄ nanoparticles. *Phys. Rev. Lett.* **1996**, *77*, 394. [[CrossRef](#)] [[PubMed](#)]
73. Berkowitz, A.E.; Kodama, R.H.; Makhlof, S.A.; Parker, F.T.; Spada, F.E.; McNiff, E.J., Jr.; Foner, S. Anomalous properties of magnetic nanoparticles. *J. Magn. Magn. Mater.* **1999**, *196–197*, 591. [[CrossRef](#)]
74. Tobia, D.; De Biasi, E.; Granada, M.; Troiani, H.E.; Zampieri, G.; Winkler, E.; Zysler, R.D. Evolution of the magnetic anisotropy with particle size in antiferromagnetic Cr₂O₃ nanoparticles. *J. Appl. Phys.* **2010**, *108*. [[CrossRef](#)]

75. Lehlooh, A.-F.; Mahmood, S.H.; Williams, J.M. On the particle size dependence of the magnetic anisotropy energy constant. *Phys. B Condens. Matter*. **2002**, *321*, 159–162. [[CrossRef](#)]
76. López-Ortega, A.; Lottini, E.; Fernández, C.D.J.; Sangregorio, C. Exploring the Magnetic Properties of Cobalt-Ferrite Nanoparticles for the Development of a Rare-Earth-Free Permanent Magnet. *Chem. Mater.* **2015**, *27*, 4048–4056. [[CrossRef](#)]
77. Néel, L. Anisotropie magnétique superficielle et surstructures d'orientation. *J. Phys.* **1954**, *15*, 225–239. [[CrossRef](#)]
78. Caizer, C. Magnetic properties of the novel nanocomposite $(\text{Zn}_{0.15}\text{Ni}_{0.85}\text{Fe}_2\text{O}_4)_{0.15}/(\text{SiO}_2)_{0.85}$ at room temperature. *J. Magn. Mater.* **2008**, *320*, 1056–1062. [[CrossRef](#)]
79. Caizer, C.; Savii, C.; Popovici, M. Magnetic behaviour of iron oxide nanoparticles dispersed in a silica matrix. *Mater. Sci. Eng. B* **2003**, *97*, 129–134. [[CrossRef](#)]
80. Hrianca, I.; Caizer, C.; Schlett, Z. Dynamic magnetic behavior of Fe_3O_4 colloidal nanoparticles. *J. Appl. Phys.* **2002**, *92*, 2125–2132. [[CrossRef](#)]
81. Kodama, R. Magnetic nanoparticles. *J. Magn. Magn. Mater.* **1999**, *200*, 359–372. [[CrossRef](#)]
82. Kneller, E.; Seeger, A.; Kronmüller, H. *Ferromagnetismus*; Springer: Berlin/Heidelberg, Germany, 1962.
83. Caizer, C.; Tura, V. Magnetic relaxation/stability of Co ferrite nanoparticles embedded in amorphous silica particles. *J. Magn. Mater.* **2006**, *301*, 513–520. [[CrossRef](#)]
84. Hergt, R.; Dutz, S. Magnetic particle hyperthermia—biophysical limitations of a visionary tumour therapy. *J. Magn. Magn. Mater.* **2007**, *311*, 187–192. [[CrossRef](#)]